JOURNAL OF SOLID STATE CHEMISTRY 37, 157–164 (1981)

Some Systematics of the Garnet Structure

F. C. HAWTHORNE

Department of Earth Sciences, University of Manitoba, Winnipeg, Manitoba, Canada, R3T 2N2

Received May 28, 1980; in final form August 20, 1980

Equations relating the positional parameters of the anion in the oxide garnets to the mean constituent ionic radii of the cations occupying the {X}, [Y], and (Z) sites have been derived from published garnet structures using multiple regression analysis:

$$x = 0.0278(22)r\ \{X\} + 0.0123(28)r\ [Y] - 0.0482(16)r(Z) + 0.0141$$
$$y = -0.0237(25)r\ \{X\} + 0.0200(32)r\ [Y] + 0.0321(18)r(Z) + 0.0523$$
$$z = -0.0102(20)r\ \{X\} + 0.0305(25)r\ [Y] - 0.0217(14)r(Z) + 0.6519$$

Variations of mean bond lengths with constituent ionic radius are examined for the garnet structures. Deviations of mean bond length from the sum of the constituent ionic radii may be correlated with the ionic radius of the cations at the other sites in the structure.

Introduction

The garnet structure is one of considerable chemical compliance, and a large number of compounds are of this structure type. Consequently the systematization of crystallographic properties within this class of materials is extremely useful. Such systematics may be used to demonstrate internal consistency of crystallographic data, to identify errors in assigned cation site-occupancies, valence states and spin states, to derive ionic radii, and to forecast the possible existence of new compounds (*1*, *2*).

A detailed description of the garnet structure and a survey of known garnet compounds is given by Geller (*3*) and a detailed discussion and systematization of silicate garnets given by Novak and Gibbs (*4*). Langley and Sturgeon (*5*) have recently related the cell edge of garnet to the ionic radii of the cations and anions comprising the structure, and have summarized previous similar studies.

Garnets have the general formula $\{X_3\}[Y_2](Z_3)\phi_{12}$ where {}, [], () denote dodecahedral, octahedral, and tetrahedral coordination respectively, and ϕ denotes the anion(s); this representation is slightly modified after Geller (*3*). The structure has the space group *Ia*3*d* and all cation positions are fixed by symmetry. The anion occupies the general position and thus has three degrees of positional freedom. Variation in the anion positional parameters may be correlated with the ionic radii of the cations and anions constituting the structures. This was done by Novak and Gibbs (*4*) for the silicate garnets, resulting in the equations:

$$x = 0.022r\ \{X\} + 0.014r\ [Y] + 0.0059$$
$$y = -0.023r\ \{X\} + 0.037r\ [Y] + 0.0505$$
$$z = -0.009r\ \{X\} + 0.034r\ [Y] + 0.6431$$

0022-4596/81/050157-08$02.00/0

TABLE I

Structural Data (Distances in Å) for 54 Oxide Garnets

	a(Å)	x	y	z	⟨X – O⟩	⟨Y – O⟩	⟨Z – O⟩	r{X}	r[Y]	r(Z)	Reference
1. $Lu_3Al_5O_{12}$	11.906(4)	0.0294(4)	0.0537(5)	0.6509(6)	2.330(4)	1.939(7)	1.760(6)	0.977	0.535	0.390	(*8*)
2. $Yb_3Al_5O_{12}$	11.931(4)	0.0296(5)	0.0529(6)	0.6504(7)	2.340(5)	1.935(8)	1.762(8)	0.985	0.535	0.390	(*8*)
3. $Y_3Al_5O_{12}$	12.000(4)	0.0306(4)	0.0512(4)	0.6500(5)	2.368(4)	1.937(6)	1.761(5)	1.019	0.535	0.390	(*8*)
4. $Gd_3Al_5O_{12}$	12.113(4)	0.0311(4)	0.0509(4)	0.6490(5)	2.397(4)	1.944(6)	1.781(5)	1.053	0.535	0.390	(*8*)
5. $Lu_3Ga_5O_{12}$	12.188(4)	0.0252(5)	0.0570(8)	0.6506(8)	2.348(6)	1.987(10)	1.852(9)	0.977	0.620	0.470	(*8*)
6. $Yb_3Ga_5O_{12}$	12.204(4)	0.0259(5)	0.0563(5)	0.6519(7)	2.355(5)	2.002(8)	1.835(7)	0.985	0.620	0.470	(*8*)
7. $Y_3Ga_5O_{12}$	12.280(4)	0.0272(2)	0.0558(3)	0.6501(3)	2.383(2)	1.995(4)	1.849(3)	1.019	0.620	0.470	(*8*)
8. $Yb_3Fe_5O_{12}$	12.302(1)	0.0263(3)	0.0570(5)	0.6506(5)	2.376(3)	2.007(5)	1.861(4)	0.985	0.645	0.490	(*8*)
9. $Y_3Fe_5O_{12}$	12.376(4)	0.0270(4)	0.0569(5)	0.6505(5)	2.395(4)	2.019(6)	1.866(5)	1.019	0.645	0.490	(*8*)
10. $Dy_3Fe_5O_{12}$	12.405(1)	0.0272(4)	0.0570(5)	0.6511(5)	2.400(4)	2.031(6)	1.864(5)	1.027	0.645	0.490	(*8*)
11. $Sm_3Fe_5O_{12}$	12.540(4)	0.0282(4)	0.0552(5)	0.6503(5)	2.442(4)	2.039(6)	1.875(5)	1.079	0.645	0.490	(*8*)
12. $Lu_3Fe_5O_{12}$	12.290(4)	0.0251(8)	0.0595(8)	0.6523(10)	2.352(7)	2.033(12)	1.867(11)	0.977	0.645	0.490	(*8*)
13. $Lu_3Fe_5O_{12}$	12.278(4)	0.0255(5)	0.0592(8)	0.6514(8)	2.356(6)	2.019(10)	1.868(8)	0.977	0.645	0.490	(*8*)
14. $Y_3Fe_5O_{12}$	12.376(1)	0.0269(1)	0.0581(3)	0.6495(1)	2.394(3)	2.012(1)	1.880(1)	1.019	0.645	0.490	(*9*)
15. $Y_3Fe_5O_{12}$	12.376(4)	0.0274(9)	0.0572(9)	0.6492(9)	2.400	2.006	1.875	1.019	0.645	0.490	(*10*)
16. $Gd_3Fe_5O_{12}$	12.470(5)	0.0269(7)	0.0550(5)	0.6478(5)	2.425(6)	2.000(8)	1.890(8)	1.053	0.645	0.490	(*11*)
17. $Y_3Fe_5O_{12}$	12.376(3)	0.0271(1)	0.0567(1)	0.6504(1)	2.397(1)	2.017(1)	1.865(1)	1.019	0.645	0.490	(*12*)
18. $Y_3[Al,Ga]_5O_{12}$	12.060(1)	0.0299(6)	0.0513(6)	0.6486(6)	2.379(4)	1.930(6)	1.787(6)	1.019	0.537	0.413	(*13*)
19. $Y_3[Al,Ga]_5O_{12}$	12.111(1)	0.0293(6)	0.0529(5)	0.6480(6)	2.377(4)	1.937(6)	1.810(6)	1.019	0.550	0.429	(*13*)
20. $Y_3[Al,Ga]_5O_{12}$	12.163(1)	0.0294(6)	0.0543(6)	0.6498(7)	2.381(4)	1.971(6)	1.808(6)	1.019	0.572	0.442	(*13*)
21. $Y_3[Al,Ga]_5O_{12}$	12.226(1)	0.0280(5)	0.0535(4)	0.6502(5)	2.387(4)	1.979(6)	1.823(6)	1.019	0.597	0.459	(*13*)
22. $Y_3[Al,Fe]_5O_{12}$	12.24(1)	0.0289(1)	0.0549(1)	0.6511(1)	2.387	1.999	1.817	1.019	0.621	0.442	(*14*)
23. $Y_3[Al,Fe]_5O_{12}$	12.24(1)	0.0289(1)	0.0549(1)	0.6511(1)	2.387	1.999	1.817	1.019	0.619	0.440	(*14*)
24. $Y_3[Al,Fe]_5O_{12}$	12.176(6)	0.0297(1)	0.0536(1)	0.6507(1)	2.385	1.980	1.798	1.019	0.593	0.421	(*14*)
25. $Y_3[Al,Fe]_5O_{12}$	12.097(8)	0.0299(1)	0.0522(1)	0.6499(1)	2.379	1.954	1.785	1.019	0.561	0.406	(*14*)
26. $Mn_3Fe_2Ge_3O_{12}$	12.087(3)	0.0299(3)	0.0539(3)	0.6531(3)	2.362(5)	1.995(7)	1.766(7)	0.960	0.645	0.390	(*15*)
27. $Ca_3Fe_2Ge_3O_{12}$	12.325(3)	0.0342(2)	0.0510(2)	0.6517(2)	2.451	2.017	1.765	1.120	0.645	0.390	(*16*)
28. $Ca_3Cr_2Ge_3O_{12}$	12.259(2)	0.0342(2)	0.0498(2)	0.6507(2)	2.445	1.990	1.759	1.120	0.615	0.390	(*17*)
29. $Ca_3Fe_2Ge_3O_{12}$	12.325(3)	0.0355	0.0528	0.6510	2.452	2.020	1.769	1.120	0.645	0.390	(*18*)
30. $Mn_3Al_2Ge_3O_{12}$	12.087	0.0314	0.0497	0.6470	2.404	1.914	1.786	0.960	0.535	0.390	(*19*)
31. Almandine	11.507(2)	0.0340(2)	0.0494(2)	0.6528(2)	2.291(1)	1.889(2)	1.634(2)	0.919	0.543	0.268	(*20*)
32. Pyrope	11.459(1)	0.0329(1)	0.0502(1)	0.6534(1)	2.269(1)	1.886(1)	1.634(1)	0.890	0.535	0.260	(*4*)
33. Cr-pyrope	11.526(1)	0.0335(1)	0.0507(1)	0.6537(1)	2.285(1)	1.905(1)	1.639(1)	0.900	0.563	0.260	(*4*)
34. Almandine	11.531(1)	0.0343(1)	0.0486(1)	0.6533(1)	2.299(1)	1.896(2)	1.628(1)	0.926	0.535	0.260	(*4*)

35. Spessartine	11.612(1)	0.0351(1)	0.0477(1)	0.6526(1)	2.328(1)	1.902(1)	1.637(1)	0.960	0.536	0.260	*(4)*
36. Mn-grossular	11.690(1)	0.0358(1)	0.0463(1)	0.6518(1)	2.353(1)	1.903(1)	1.645(1)	1.019	0.536	0.260	*(4)*
37. Grossular	11.845(1)	0.0381(1)	0.0449(1)	0.6514(1)	2.405(1)	1.924(1)	1.645(1)	1.118	0.538	0.260	*(4)*
38. Uvarovite	11.988(1)	0.0399(2)	0.0474(2)	0.6535(2)	2.430(1)	1.985(2)	1.643(2)	1.119	0.608	0.260	*(4)*
39. Goldmanite	12.011(1)	0.0385(2)	0.0474(2)	0.6539(2)	2.425(2)	1.988(2)	1.655(2)	1.113	0.616	0.260	*(4)*
40. Andradite	12.058(1)	0.0397(2)	0.0489(1)	0.6556(2)	2.433(1)	2.024(2)	1.643(2)	1.118	0.644	0.260	*(4)*
41. Berzeliite	12.355(2)	0.0391(3)	0.0522(3)	0.6568(3)	2.471(4)	2.098(4)	1.694(4)	1.140	0.737	0.335	*(21)*
42. $\{Y,Pr\}_3(Sc,Fe)_5O_{12}$	12.439	0.0272(6)	0.0575(6)	0.6515(6)	2.403(5)	2.044(9)	1.868(8)	1.020	0.685	0.490	*(22)*
43. $\{Y,Pr\}_3(Sc,Fe)_5O_{12}$	12.518	0.0262(4)	0.0565(4)	0.6517(5)	2.417(4)	2.053(6)	1.882(6)	1.044	0.685	0.490	*(22)*
44. $\{Y,Pr\}_3(Sc,Fe)_5O_{12}$	12.639	0.0283(3)	0.0545(3)	0.6521(3)	2.460(3)	2.073(5)	1.871(4)	1.090	0.694	0.490	*(22)*
45. $\{Y,Pr\}_3(Sc,Fe)_5O_{12}$	12.737	0.0290(4)	0.0545(4)	0.6513(4)	2.485(4)	2.081(5)	1.886(5)	1.126	0.692	0.490	*(22)*
46. $Ca_3(Fe,Ti,Si)_5O_{12}$	12.240(1)	0.0352(2)	0.0489(2)	0.6508(2)	2.451	1.988	1.744	1.120	0.624	0.360	*(23)*
47. $\{Bi,Ca\}_3(Fe,V)_5O_{12}$	12.470(4)	0.0339(2)	0.0524(2)	0.6512(2)	2.473(3)	2.039(6)	1.799(2)	1.121	0.645	0.424	*(24)*
48. $NaCa_2Co_2V_3O_{12}$	12.430(3)	0.0382(4)	0.0514(6)	0.6551(7)	2.487(8)	2.086(10)	1.722(11)	1.140	0.745	0.355	*(25)*
49. $Na_3Sc_2V_3O_{12}$	12.602(4)	0.0418	0.0486	0.6540	2.557	2.106	1.714	1.180	0.745	0.355	*(26)*
50. Grossular	11.874(4)	0.0389(5)	0.0456(5)	0.6524(5)	2.411	1.945	1.638	1.107	0.560	0.263	*(27)*
51. Pyrope	11.459	0.034	0.050	0.654	2.276	1.896	1.620	0.890	0.535	0.260	*(28)*
52. Grossular	11.855(1)	0.0383(1)	0.0456(1)	0.6513(1)	2.405(1)	1.926(1)	1.650(1)	1.117	0.552	0.260	*(29)*
53. $\{Y,Bi\}_3Fe_5O_{12}$	12.531	0.0279(7)	0.0548(7)	0.6571(7)	2.436(6)	2.051(10)	1.863(9)	1.114	0.645	0.490	*(30)*
54. $\{Bi,Ca\}_3Fe_2(Fe,V)_3O_{12}$	12.489	0.0334(1)	0.0520(2)	0.6519(2)	2.473(2)	2.048(3)	1.798(3)	1.126	0.645	0.430	*(30)*

Unit formulae: 18, $Y_3Ga_{1.03}Al_{3.97}O_{12}$; 19, $Y_3Ga_{1.92}Al_{3.08}O_{12}$; 20, $Y_3Ga_{2.90}Al_{2.10}O_{12}$; 21, $Y_3Ga_{4.08}Al_{0.92}O_{12}$; 22, $Y_3Fe_{3.14}Al_{1.86}O_{12}$; 23, $Y_3Fe_{3.03}Al_{1.97}O_{12}$; 24, $Y_3Fe_{2.04}Al_{2.96}O_{12}$; 25, $Y_3Fe_{1.01}Al_{3.99}O_{12}$; 31, $\{Ca_{0.05}Fe^{2+}_{2.39}Mg_{0.55}\}[Fe^{3+}_{0.14}Al_{1.89}Ti_{0.02}](Al_{0.10}Fe^{3+}_{0.08}Si_{2.83}P_{0.01})O_{12}$; 32, $Mg_3Al_2Si_3O_{12}$; 33, $\{Mg_{2.63}Fe^{2+}_{0.27}Ca_{0.09}Mn_{0.01}\}$ $[Al_{1.34}Fe^{3+}_{0.09}Cr_{0.57}]Si_3O_{12}$; 34, $\{Fe_{2.59}Mg_{0.27}Ca_{0.13}Mn_{0.01}\}Al_{1.98}Si_3O_{12}$; 35, $\{Mn_{2.58}Fe_{0.34}Ca_{0.08}\}[Al_{1.99}Fe_{0.01}]Si_3O_{12}$; 36, $\{Ca_{1.34}Mn_{0.81}Fe_{0.76}Mg_{0.09}\}$ $[Al_{1.99}Ti_{0.01}]Si_3O_{12}$; 37, $\{Ca_{2.96}Mn_{0.04}\}[Al_{1.95}Fe_{0.05}]Si_3O_{12}$; 38, $\{Ca_{2.99}Mn_{0.01}\}[Cr_{1.73}Al_{0.21}Fe_{0.05}Ti_{0.01}]Si_3O_{12}$; 39, $\{Ca_{2.90}Mn_{0.02}Mg_{0.08}\}[V_{1.20}Al_{0.47}Fe_{0.33}]Si_3O_{12}$; 40, $\{Ca_{2.97}Mg_{0.02}Mn_{0.01}\}[Fe_{1.99}Al_{0.01}]Si_3O_{12}$; 41, $\{NaCa_2\}[Mg_{1.70}Mn_{0.30}]As_3O_{12}$; 42, $\{Y_{2.97}Pr_{0.03}\}[Sc_{0.8}Fe_{1.2}]Fe_3O_{12}$; 43, $\{Y_{2.30}Pr_{0.70}\}[Sc_{0.8}Fe_{1.2}]Fe_3O_{12}$; 44, $\{Y_{1.00}Pr_{2.00}\}[Sc_{0.97}Fe_{1.03}]Fe_3O_{12}$; 45, $Pr_3[Sc_{0.94}Fe_{1.06}]Fe_3O_{12}$: 46, $Ca_3Fe_2(Ti_{1.42}Si_{1.58})O_{12}$; 47, $\{Ca_{2.92}Bi_{0.08}\}(Fe_{3.54}V_{1.46})O_{12}$; 50, $\{Ca_{2.82}Mg_{0.18}\}[Al_{1.62}Ti_{0.02}Fe^{3+}_{0.25}Mg_{0.11}](Al_{0.6}Si_{2.94})O_{12}$; 51, $Mg_3Al_2Si_3O_{12}$; 52, $\{Ca_{2.96}Mg_{0.04}\}[Al_{1.77}Fe^{3+}_{0.13}Mn_{0.01}Mg_{0.09}]Si_3O_{12}$; 53, $\{Y_{1.12}Bi_{1.88}\}Fe_5O_{12}$; 54, $\{Bi_{0.34}Ca_{2.66}\}Fe^{3+}_2(Fe^{3+}_{1.67}V_{1.33})O_{12}$.

where the ionic radii used were those of Shannon and Prewitt (*6*). In the present study, analogous equations are developed for the whole class of oxide garnets; fluoride garnets are not considered as only the cryolithionite structure (*7*) is known in detail.

Analysis of Observed Garnet Structures

The present study was based on 49 reasonably precise structure refinements of oxide garnets, pertinent data from which is assembled in Table I, where they are grouped together according to the identity of the (Z) cation. Several additional structures are also listed in Table I. Some of these are older refinements which have been superceded by more recent work; the others were used as a test of the resultant equations (Table III). Ionic radii are taken from Shannon (*32*). Multiple regression analyses were performed on the positional parameters and the mean ionic radii of the {X}, [Y], and (Z) cations, respectively, with the positional parameters as dependent variables. One specific garnet listed in Table I exhibited the maximum deviation for all three regression equations, and these deviations were considerably larger than those exhibited by the rest of the data set. The relevant values for this garnet, $Mn_3Al_2Ge_3O_{12}$, (number 31 in Table I) are: x-obs. = 0.0314, calc. = 0.0288; y-obs. = 0.0497, calc. = 0.0526; z-obs. = 0.6470, calc. = 0.6498. This suggests that the positional parameters for this garnet are considerably in error, and shows the utility of this approach in isomorphous groups of structures. Note that the unit cell parameter given for $Mn_3Al_2Ge_3O_{12}$ in Table I is not compatible with previous determinations (11.902 Å—(*3*)). The multiple regression analyses were repeated, omitting the data for $Mn_3Al_2Ge_3O_{12}$; the results are given in Table II. The mean deviations between the observed and calculated parameters are 0.0005, 0.0007, and 0.0005 for x, y, and z, respectively. Table III shows a comparison of observed and calculated positional and unit cell parameters for a typical selection of precisely determined garnet structures. The good agreement suggests that a difference of $>2.5\sigma$ (σ = pooled standard deviation) between observed and calculated positional parameters in garnet refinements indicates significant error in the structure refinements; such is the case for $Mn_3Al_2Ge_3O_{12}$ and $Na_3Sc_2V_3O_{12}$ (using estimated σ's of 0.0005 for the observed positional parameters).

The prediction of cell parameters from

TABLE II

RESULTS OF MULTIPLE LINEAR REGRESSION ANALYSES

Dependent variable	Independent variable	Slope	Intercept	Correlation coefficient	$\|t\|^a$
x	r{X}	0.0278(22)			12.6
	r[Y]	0.0123(28)	0.0141	0.985	4.4
	r(Z)	−0.0482(16)			29.9
y	r{X}	−0.0237(25)			9.6
	r[Y]	0.0200(32)	0.0523	0.969	6.3
	r(Z)	0.0321(18)			17.8
z	r{X}	−0.0102(20)			5.1
	r[Y]	0.0305(25)	0.6519	0.924	12.0
	r(Z)	−0.0217(14)			14.9

[a] t is the Student statistic for the slope.

the linear regression equations of Novak and Colville (*31*) and Langley and Sturgeon (*5*) is less successful (Table III). It is apparent that the cell parameter cannot be accurately expressed as a linear function of the constituent cation radii in the garnet group as a whole.

TABLE III

COMPARISON OF OBSERVED AND CALCULATED PARAMETERS FOR SELECTED GARNETS

		$Y_3Fe_5O_{12}$	$Ca_3Fe_2Ge_3O_{12}$	Pyrope	Berzeliite	$NaCa_2Co_2V_3O_{12}$	$\{Y_{1.12}Bi_{1.88}\}Fe_5O_{12}$	$\{Bi_{0.34}Ca_{2.66}\}Fe_2(Fe_{1.67}V_{1.33})O_{12}$
Observed	x	0.0271(1)	0.0342(2)	0.0329(1)	0.0391(3)	0.0382(4)	0.0279(7)	0.0334(2)
	y	0.0567(1)	0.0510(2)	0.0502(1)	0.0522(3)	0.0514(6)	0.0548(7)	0.0520(2)
	z	0.6504(1)	0.6517(2)	0.6534(1)	0.6568(3)	0.6551(7)	0.6517(5)	0.6519(2)
	a	12.376(3)	12.325(3)	11.459(1)	12.355(2)	12.430(3)	12.531	12.489
Calculated	x	0.0268	0.0344	0.0329	0.0388	0.0379	0.0294	0.0326
	y	0.0568	0.0512	0.0503	0.0508	0.0516	0.0545	0.0523
	z	0.6505	0.6517	0.6535	0.6555	0.6553	0.6496	0.6508
	a^a	12.373	12.359	11.527	12.442	12.493	12.539	12.446
	a^b	12.384	12.338	11.470	12.417	12.474	12.545	12.435

[a] Calculated from the equation of Langley and Sturgeon (*5*).

[b] Calculated from the equation of Novak and Colville (*31*).

Structural Variation in Garnets

In many groups of isomorphous structures, the variation in the mean bond lengths of cation polyhedra may be related to the mean ionic radius of the cations occupying the sites. Novak and Gibbs (*4*) have shown that the variations in $\langle X - O \rangle$ and $\langle Y - O \rangle$ are linear functions of $r\{X\}$ and $r[Y]$ in the silicate garnets. Mean bond length-constituent ionic radius relationships for the garnets of Table I are shown in Fig. 1. The solid lines in the diagram are not regression lines but show the mean bond length forecast from the sum of the cation and anion radii. The agreement is fairly close for tetrahedral coordination but the scatter increases significantly with increasing coordination number. These deviations from a "hard-sphere" model are not random, but seem to be related to the mean ionic radii of the cations occupying the other cation sites; this is most apparent for the dodecahedrally coordinated site (Fig. 1). Using the equations of Table I and the cell parameter equation of Langley and Sturgeon (*5*), this effect may be examined systematically by generating calculated structures and examining mean bond length variations with the mean constituent ionic radius for two of the cation sites held constant. The results of such a procedure lead to the bond length–ionic radius relationships of Fig. 2. This figure shows for each site, the mean bond length–constituent cation radius curves for specific constant values of the constituent cation radius for the other two sites; in addition, the ideal "hard sphere" model ($\langle M - O \rangle = r_{\text{cation}} +$

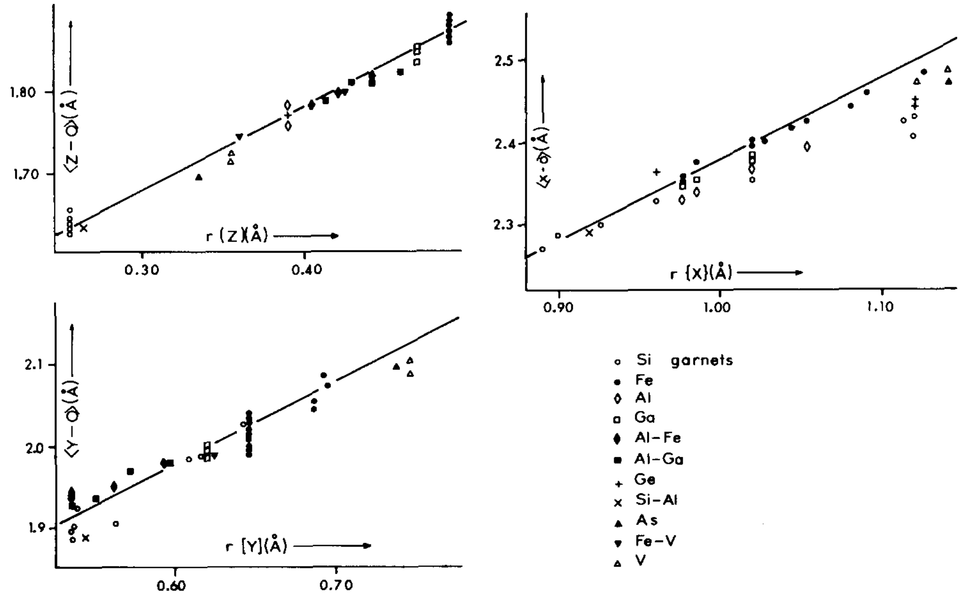

FIG. 1. Mean bond length vs constituent cation radius for the {X}, [Y], and (Z) sites in garnets. The heavy lines correspond to additivity of ionic radii.

r_{anion}) is marked. These ideal curves bear a marked similarity to those of the real structures in Fig. 1. This is hardly surprising as the predictive curves were derived from the real structures. However, they do illustrate the inductive effect that the cations occupying two of the sites have on the mean bond length of the remaining cation(s). Data for the silicate and REE iron garnets are shown on the ⟨X − O⟩ vs $r\{X\}$ curve to illustrate the trends of the data. The data does not exactly follow the trends derived from the calculated structures; this occurs because the equation for the cell constant leads to considerable error for certain values of constituent cation radius.

It is apparent from Figure 2 that variation in r(Z) has only a slight effect on ⟨X − O⟩. Ignoring this effect for ⟨X − O⟩, the ⟨X − O⟩ vs $r\{X\}$ relationship can be considered as contoured for $r[Y]$. Thus all synthesized garnets may be plotted on this figure if $r\{X\}$ and $r\langle\{Y\}$ (i.e., the site-occupancies) are known. This results in Fig. 3; not all garnets have been plotted, but enough are shown to indicate the salient features. Although individual garnet series trend across the ideal "hard sphere" model relationship, the garnets as a whole tend to follow an overall trend that is parallel to the ideal "hard sphere" model relationship; stable garnets exhibit $r\{X\}$ and $r[Y]$ values that do not lead to too great a deviation from the ideal "hard sphere" model for mean bond length. The position of the data points plotted in Fig. 3 is only approximate; however, if it is assumed that the cell parameter equation will forecast a to within ±0.1 Å, the data points of Fig. 3 should be within ±0.02 Å. Thus the overall trend of Fig. 3 should not be significantly affected by any errors in the model structure calculations.

Shannon (*32, 33*) has reviewed factors that affect deviations of mean bond lengths from additivity of ionic radii; these factors are associated with specific bonding effects. This does not seem to be the case in the present situation, where such deviations are correlated solely with the size of the cations occupying the remaining sites in

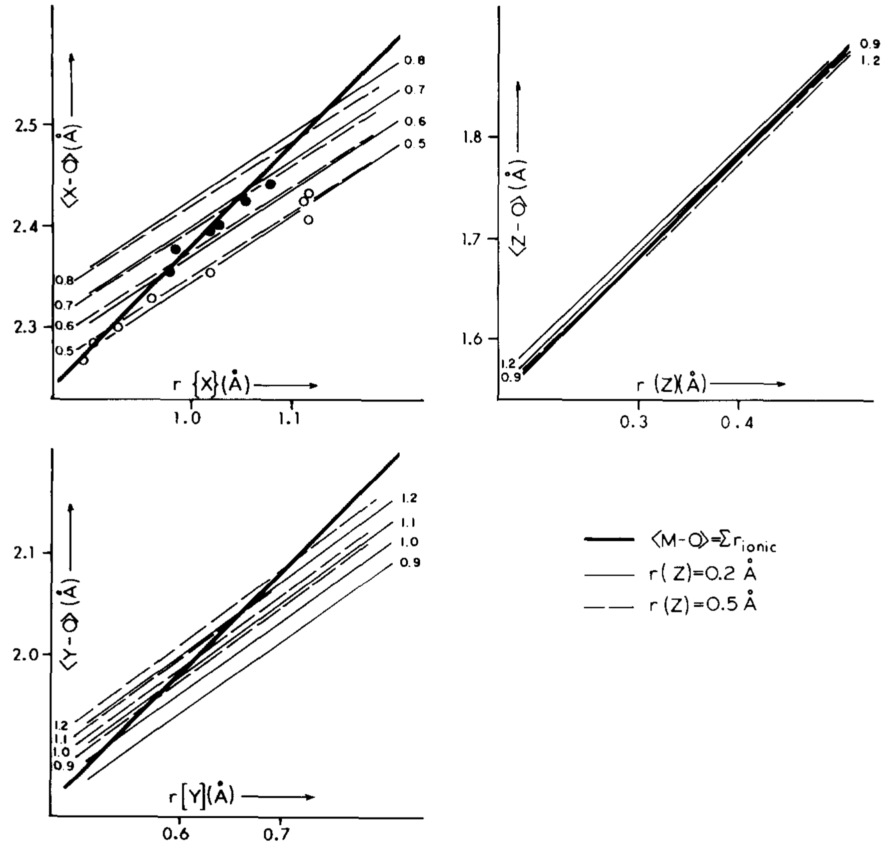

FIG. 2. The variation of mean bond length with constituent cation radius for the three sites of the garnet structure. The heavy lines denote the sum of the cation and anion radii. The light lines denote the cation radii values (at the other sites) used to calculate the atomic coordinates and cell parameter from which the mean bond lengths were calculated. For the {X} and [Y] sites, the full and broken lines are for $r(Z) = 0.2$ and 0.5 Å, respectively, and the values marked on the graphs are the values of $r[Y]$ and $r\{X\}$, respectively. For the (Z) site, the full and broken lines are for $r[Y] = 0.5$ and 0.8 Å, respectively, with the $r\{X\}$ values marked on the figure.

the structure. The results given above suggest that for specific values of two of the cation radii, there is an optimum value for the third, where the mean bond length at the third site approximates the sum of the ionic radii. Cations larger and smaller than this optimum value may occupy the site but the mean bond length will show deviations from the additivity relationship. A simple model of compression and distension for negative and positive deviations, respectively, would seem to be appropriate. However, in this case one would expect the compressibility of the garnet to be positively correlated with negative deviations from the additivity relationship. The Al octahedra in pyrope and grossular have deviations from additivity of −0.029 and 0.006 Å, respectively; however, Hazen and Finger (*34*) give the polyhedral bulk modulus for [Al] in both pyrope and grossular as 2200 (500) kbar. This result suggests that a simple model of polyhedral compression/distension is not applicable, un-

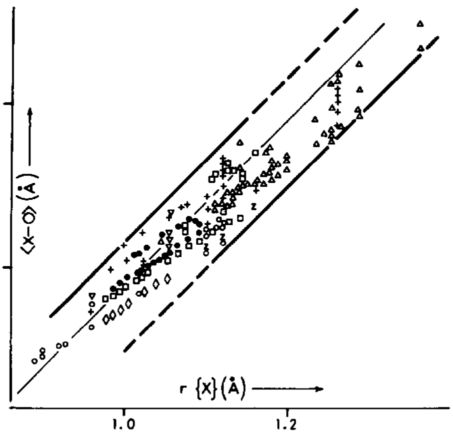

FIG. 3. The calculated relationship between ⟨X − O⟩ and $r\{X\}$ contoured for $r[Y]$, ignoring the small effect of $r(Z)$ on this particular relationship. Synthesized garnets are plotted on this figure using their $r\{X\}$ and $r[Y]$ values. The central line corresponds to additivity of constituent ionic radii and the heavy outer lines mark the approximate limits of known garnet compositions. Note the parallelism between the additivity relationship and the compositional limits.

less the differences in compressibility are less than the standard deviation of the bulk modulus.

Acknowledgments

The author would like to express his gratitude to Dr. R. B. Ferguson for his support during this study, and his thanks to an anonymous referee for his pertinent comments.

References

1. R. J. HILL, J. R. CRAIG, AND G. V. GIBBS, *Phys. Chem. Minerals* **4,** 317 (1979).
2. F. K. LOTGERING AND R. P. VAN STAPELE, *Mater. Res. Bull.* **3,** 507 (1968).
3. S. GELLER, *Z. Kristallogr.* **125,** (1967).
4. G. A. NOVAK AND G. V. GIBBS, *Amer. Mineral.* **56,** 791 (1971).
5. R. H. LANGLEY AND G. D. STURGEON, *J. Solid State Chem.* **30,** 79 (1979).
6. R. D. SHANNON AND C. T. PREWITT, *Acta Crystallogr.* **B25,** 925 (1969).
7. S. GELLER, *Amer. Mineral.* **56,** 18 (1971).
8. F. EULER AND J. A. BRUCE, *Acta Crystallogr.* **10,** 971 (1965).
9. A. BATT AND B. POST, *Acta Crystallogr.* **15,** 1268 (1962).
10. S. GELLER AND M. A. GILLEO, *J. Phys. Chem. Solids* **3,** 30 (1957).
11. J. E. WEIDENBORNER, *Acta Crystallogr.* **14,** 1051 (1961).
12. M. BONNET, A. DELAPALME, H. FUESS, AND M. THOMAS, *Acta Crystallogr.* **B31,** 2233 (1975).
13. M. MAREZIO, J. P. REMEIKA, AND P. D. DERNIER, *Acta Crystallogr.* **B24,** 1670 (1968).
14. P. FISCHER, W. HÄLG, P. ROGGWILLER, AND E. R. CZERLINSKY, *Solid State Commun.* **16,** 987 (1975).
15. M. D. LIND AND S. GELLER, *Z. Kristallogr.* **129,** 427 (1969).
16. W. PRANDL, *Solid State Commun.* **10,** 529 (1972).
17. W. PRANDL, *Solid State Commun.* **11,** 645 (1972).
18. R. PLUMIER, *Solid State Commun.* **10,** 5 (1972).
19. R. PLUMIER, *Solid State Commun.* **12,** 109 (1973).
20. W. PRANDL, *Z. Kristallogr.* **134,** 333 (1971).
21. F. C. HAWTHORNE, *Acta Crystallogr.* **B32,** 1581 (1976).
22. P. D. DERNIER, E. M. GYORGY, AND W. H. FRODKIEWICZ, *J. Solid State Chem.* **10,** 122 (1974).
23. H. P. WEBER, D. VIRGO, AND F. E. HUGGINS, *Carnegie Inst. Wash. Year Book* **74,** 575 (1975).
24. E. L. DUKHOVSKAYA AND YU. G. SAKSONOV, *Sov. Phys. Solid State* **10,** 2613 (1969).
25. E. L. DUKHOVSKAYA AND B. V. MILL, *Sov. Phys. Crystallogr.* **19,** 47 (1974).
26. E. L. BELOKONEVA, B. V. MILL, M. A. SIMONOV, AND N. V. BELOV, *Sov. Phys. Crystallogr.* **19,** 228 (1974).
27. S. C. ABRAHAMS AND S. GELLER, *Acta Crystallogr.* **11,** 437 (1958).
28. A. ZEMANN AND J. ZEMANN, *Acta Crystallogr.* **14,** 835 (1961).
29. W. PRANDL, *Z. Kristallogr.* **123,** 81 (1966).
30. S. GELLER AND A. A. COLVILLE, *AIP Conf. Proc. No. 24, Magnetism and Magnetic Materials,* 372 (1974).
31. G. A. NOVAK AND A. A. COLVILLE, *in* "Abstr. Cordilleran Sect., Southwest Geol. Soc. Amer. Prog. 1975."
32. R. D. SHANNON, *Acta Crystallogr.* **A32,** 751 (1976).
33. R. D. SHANNON, "NATO Adv. Study Inst. Petrophysics" (R. G. J. Strens, ed.) (1975).
34. R. M. HAZEN AND L. W. FINGER, *Amer. Mineral.* **63,** 297 (1978).